Trypsin and Forskolin Decrease the Sensitivity of L-Type Calcium Current to Inhibition by Cytoplasmic Free Calcium in Guinea Pig Heart Muscle Cells

Yongdong You, Dieter J. Pelzer, and Siegried Pelzer
Membrane Transport and Signaling Group, Department of Physiology and Biophysics, Dalhousie University, Halifax, Nova Scotia B3H 4H7, Canada

ABSTRACT A key feature of trypsin action on ionic membrane currents including L-type Ca^{2+} current (I_{Ca}) is the removal of inactivation upon intracellular application. Here we report that trypsin also occludes the resting cytoplasmic free Ca^{2+} ($[Ca^{2+}]_i$)-induced inhibition of peak I_{Ca} in isolated guinea pig ventricular cardiomyocytes, using the whole-cell patch clamp in combination with the Fura-2 ratio-fluorescence technique. The effectiveness of trypsin to guard I_{Ca} against $[Ca^{2+}]_i$-induced inhibition was compared with that of forskolin, as cAMP-dependent phosphorylation had been suggested to confer protection against $[Ca^{2+}]_i$-induced inactivation. Intracellular dialysis of trypsin (1 mg/ml) augmented I_{Ca} by 7.2-fold, significantly larger than the threefold increase induced by forskolin (3 μM). Forskolin application after trypsin dialysis did not further enhance I_{Ca}. An increase in $[Ca^{2+}]_i$ from resting levels (varied by 0.2, 10, and 40 mM EGTA dialysis) to submicromolar concentrations after replacement of external Na^+ (Na_o^+) with tetraethylammonium (TEA^+) resulted in monotonic inhibition of control I_{Ca}, elicited from a holding potential of −40 mV at 22°C. After trypsin dialysis, however, I_{Ca} became less sensitive to submicromolar $[Ca^{2+}]_i$; the $[Ca^{2+}]_i$ of half-maximal inhibition ($K_{0.5}$, normally around 60 nM) increased by ~20-fold. Forskolin also increased the $K_{0.5}$ by ~threefold. These and accompanying kinetic data on I_{Ca} decay are compatible with a model in which it is assumed that Ca^{2+} channels can exist in two modes (a high open probability "willing" and a low open probability "reluctant" mode) that are in equilibrium with one another. An increase in $[Ca^{2+}]_i$ places a larger fraction of channels in the reluctant mode. This interconversion is hindered by cAMP-dependent phosphorylation and becomes nearly impossible after tryptic digestion.

INTRODUCTION

An important observation lending credence to the "ball-and-chain" theory of voltage-dependent inactivation of ionic channels is removal of inactivation by intracellular application of proteases. Armstrong and colleagues (1973) demonstrated removal of Na^+ channel inactivation by pronase in squid giant axons; others have successfully utilized pronase or trypsin for the same purpose in a variety of cells (see McDonald et al., 1994). Intracellular trypsin also removes the fast inactivation process in *Shaker* K^+ channels (Hoshi et al., 1990, 1991) and irreversibly activates muscarinic K^+ channels in atrial cardiomyocytes, perhaps by disrupting an inhibitory gating mechanism (Kirsch and Brown, 1989). The effects of proteases on muscle L-type Ca^{2+} channels seem to be even more complex than their actions on Na^+ and K^+ channels, as Ca^{2+} channel inactivation jointly depends on membrane potential and $[Ca^{2+}]_i$ (cf. McDonald et al., 1994). Obejero-Paz et al. (1991), for example, reported that dialysis of cultured A7r5 smooth muscle cells with trypsin abolished the (voltage-dependent) inactivation of I_{Ba} and the slow inactivation phase of I_{Ca}; the fast component of I_{Ca} inactivation was unchanged, suggesting little effect on Ca^{2+}-dependent inactivation. In contrast, Hescheler and Trautwein (1988) showed in single guinea pig ventricular heart cells that although the amplitude-enhancing effect of trypsin was equally apparent with Ba^{2+} as the charge carrier, the inactivation rate of I_{Ba} was unaffected, suggesting that the slowing of both fast and slow I_{Ca} inactivation was due to removal of Ca^{2+}-dependent inactivation. Trypsin-modified I_{Ca} was also insensitive to cAMP-dependent phosphorylation (Hescheler and Trautwein, 1988).

The primary objective of the present study was to investigate whether trypsin dialysis occludes $[Ca^{2+}]_i$-induced inhibition of I_{Ca} amplitude (cf. You et al., 1994), which would be a consequence of removal of Ca^{2+}-dependent inactivation. To this end, we performed simultaneous measurements of I_{Ca} (whole-cell patch-clamp method) and $[Ca^{2+}]_i$ (Fura-2 ratio-fluorescence technique), under control conditions and after trypsin dialysis, in cardiomyocytes enzymatically isolated from guinea pig ventricles. $[Ca^{2+}]_i$ was changed between <10 and ~2000 nM by varying the Ca^{2+} buffering capacity of the cell dialysate and by replacing external Na^+ (Na_o^+) with tetraethylammonium (TEA^+). Cell dialysis with trypsin increased peak I_{Ca} by 7.2-fold and rendered peak I_{Ca} insensitive to subsequent forskolin application. Trypsin-modified peak I_{Ca} was ~20 times less sensitive to $[Ca^{2+}]_i$ elevation than control I_{Ca} was. In addition, trypsin dialysis also compromised I_{Ca} inactivation and abolished its dependence on $[Ca^{2+}]_i$. We then compared the effectiveness of trypsin to guard I_{Ca}

Received for publication 10 May 1995 and in final form 14 August 1994.
Address reprint requests to Siegried Pelzer, Department of Physiology and Biophysics, Sir Charles Tupper Medical Building, Room 4D1, Dalhousie University, Halifax, Nova Scotia B3H 4H7, Canada. Tel.: 902-494-2555; Fax: 902-423-5956; E-mail: spelzer@tupphysiol1.bp.dal.ca

0006-3495/95/11/1838/00 $2.00

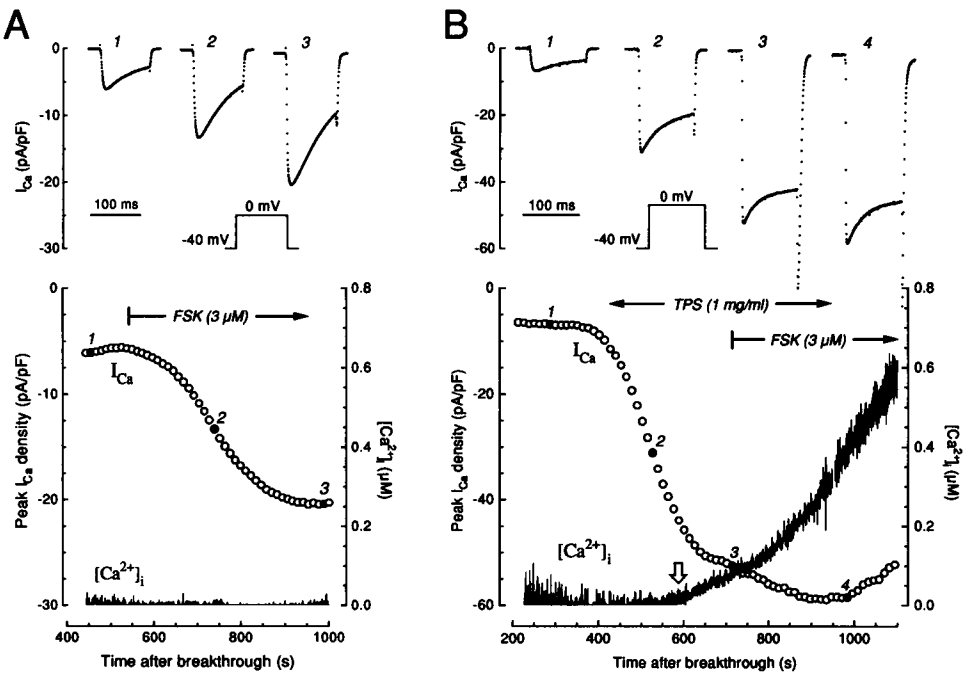

FIGURE 1 Effects of bath application of forskolin (FSK, *A*) and intracellular dialysis of trypsin (TPS, *B*) on I_{Ca} and $[Ca^{2+}]_i$. Top panels illustrate example I_{Ca} records (calibrated as current densities) during different stages of the experiment, the peak amplitudes of which are marked by ● in the time courses of peak I_{Ca} shown in the bottom panels. Also shown in the bottom panels are the concomitant $[Ca^{2+}]_i$ changes as measured by Fura-2 ratio-fluorescence. The open arrow (⇩) in B marks the onset of the $[Ca^{2+}]_i$ increase. Intracellular solution: IS-C. (*A*) Cell Aug24B, cell capacitance 188.9 pF, access resistance 5.2 MΩ; (*B*) cell Oct04C, cell capacitance 99.7 pF, access resistance 6.0 MΩ.

against $[Ca^{2+}]_i$-induced inhibition with that of forskolin, as cAMP-dependent phosphorylation has been suggested to confer protection against $[Ca^{2+}]_i$-induced inactivation (Hadley and Lederer, 1991). Bath application of forskolin augmented peak I_{Ca} by threefold. In contrast to trypsin, forskolin-stimulated peak I_{Ca} was only ~3 times less sensitive to an increase in $[Ca^{2+}]_i$ than control I_{Ca} was.

MATERIALS AND METHODS

Cell preparation and solutions

Ventricular myocytes were enzymatically isolated from hearts of male guinea pigs and stored in "KB medium," as previously described (You et al., 1994). After an aliquot of the KB medium containing myocytes was transferred to the experimental chamber positioned on top of an inverted microscope stage (Olympus IMT-2, Tokyo, Japan), cells were initially superfused with control Tyrode's solution (Tyrode) containing 140 mM NaCl, 5.4 mM KCl, 1.8 mM $CaCl_2$, 1.0 mM $MgCl_2$, 10 mM HEPES, and 10 mM glucose (pH 7.4 with NaOH). After 5 min, the superfusate was changed to K^+-free Tyrode (KCl replaced by CsCl). After giga-ohm seal formation and patch breakthrough, cells were dialyzed with one of the following intracellular solutions (IS): IS-A containing 50 mM CsCl, 80 mM Cs-aspartate, 10 mM HEPES, 6 mM $MgCl_2$, 4 mM Na_2-ATP, 0.5 mM Na-GTP, and 10 mM EGTA; IS-B containing 50 mM CsCl, 100 mM Cs-aspartate, 10 mM HEPES, 2 mM $MgCl_2$, 4 mM Mg-ATP, and 0.2 mM EGTA; or IS-C being modified from IS-B by increasing EGTA to 40 mM and reducing Cs-aspartate to 40 mM (pH 7.2 with CsOH in all cases). Na_5-Fura-2 (50 μM) (Calbiochem, San Diego, CA) and Trypsin III (1 mg/ml) (Sigma, St. Louis, MO) were added to the cell dialysate before the experiment. Na^+-free Tyrode was prepared by replacing Na^+ in K^+-free Tyrode with equimolar TEA^+. Forskolin (3 μM) (Calbiochem) was prepared from a 10 mM dimethyl sulfoxide stock solution. Experiments were performed at 22 ± 1°C.

Electrophysiology and $[Ca^{2+}]_i$ measurements

Voltage clamp was applied with an EPC9 patch-clamp amplifier (HEKA, Lambrecht/Pfalz, Germany) using the whole-cell configuration of the patch-clamp technique (Hamill et al., 1981). Briefly, I_{Ca} was evoked by 100-ms clamp pulses from −40 mV to 0 mV applied at 0.08 Hz. Cell capacitance was monitored and updated with each depolarizing pulse. The average size of the 30 cells studied was 132 ± 7 pF. All experimental data are given as mean ± SEM (n = number of cells). $[Ca^{2+}]_i$ was measured by means of the Fura-2 ratio-fluorescence method using the Deltascan-4000 system (Photon Technology International, South Brunswick, NJ). Further details are described elsewhere (You et al., 1994).

RESULTS

Effects of forskolin and trypsin on peak I_{Ca}

Bath application of the adenylate cyclase activator forskolin (Fig. 1 *A*) or intracellular dialysis of trypsin (Fig. 1 *B*) both potentiated peak I_{Ca}. A saturating concentration of forskolin (3 μM) increased peak-I_{Ca} density by 2.96 ± 0.31-fold (total n = 12; n = 7 with 0.2 mM EGTA (IS-B) and n = 5 with 40 mM EGTA (IS-C)), significantly less ($p < 0.0001$, t-test) than the 7.20 ± 0.89-fold increase recorded during cell dialysis with 1 mg/ml trypsin (total n = 6; n = 3 with 10 mM EGTA (IS-A) and n = 3 with 40 mM EGTA (IS-C)). External application of 3 μM forskolin after maximally effective dialysis with trypsin (1 mg/ml) did not further increase peak I_{Ca} (e.g., Fig. 1 *B*; 7.13 ± 1.19-fold, n = 3), suggesting that trypsin may have cleaved the C-terminal cAMP-dependent phosphorylation sites of the Ca^{2+} channel (cf. Mikami et al., 1989). A high EGTA dialysate (40 mM, IS-C) was used in the experiments of Fig. 1 to prevent Ca^{2+} overload. Although good control of $[Ca^{2+}]_i$ was achieved in the forskolin experiments (Fig. 1 *A*), $[Ca^{2+}]_i$ started to increase in the trypsin experiments, when peak I_{Ca} reached ~80% of its maximal size (⇩ in Fig. 1 *B*).

Effect of $[Ca^{2+}]_i$ elevation on forskolin- and trypsin-modified peak I_{Ca}

As reported previously (You et al., 1994), elevation of $[Ca^{2+}]_i$ at 22°C resulted in a monotonic decline of I_{Ca}. To investigate the impact of forskolin and trypsin on this $[Ca^{2+}]_i$-induced inhibition of I_{Ca}, we compared the sensitivity of peak I_{Ca} to $[Ca^{2+}]_i$ in control, forskolin-superfused, and trypsin-dialyzed cells (Fig. 2). $[Ca^{2+}]_i$ was elevated by replacing Na^+_o with TEA^+. Under control conditions, an elevation of $[Ca^{2+}]_i$ to ~300 nM resulted in an inhibition of peak I_{Ca} of ~55% (Fig. 2 *A*). Peak I_{Ca} inhibition by a slightly larger increase in $[Ca^{2+}]_i$ was less pronounced after stimulation of current with 3 μM forskolin (cf. current trace 4 and corresponding $[Ca^{2+}]_i$ in Fig. 2 *B*). I_{Ca} amplitude was still substantial during the subsequent period of spontaneous Ca^{2+} release from the sarcoplasmic reticulum (cf. current trace 5 and corresponding $[Ca^{2+}]_i$ in Fig. 2 *B*), a condition during which basal I_{Ca} usually approaches zero (see Fig. 1

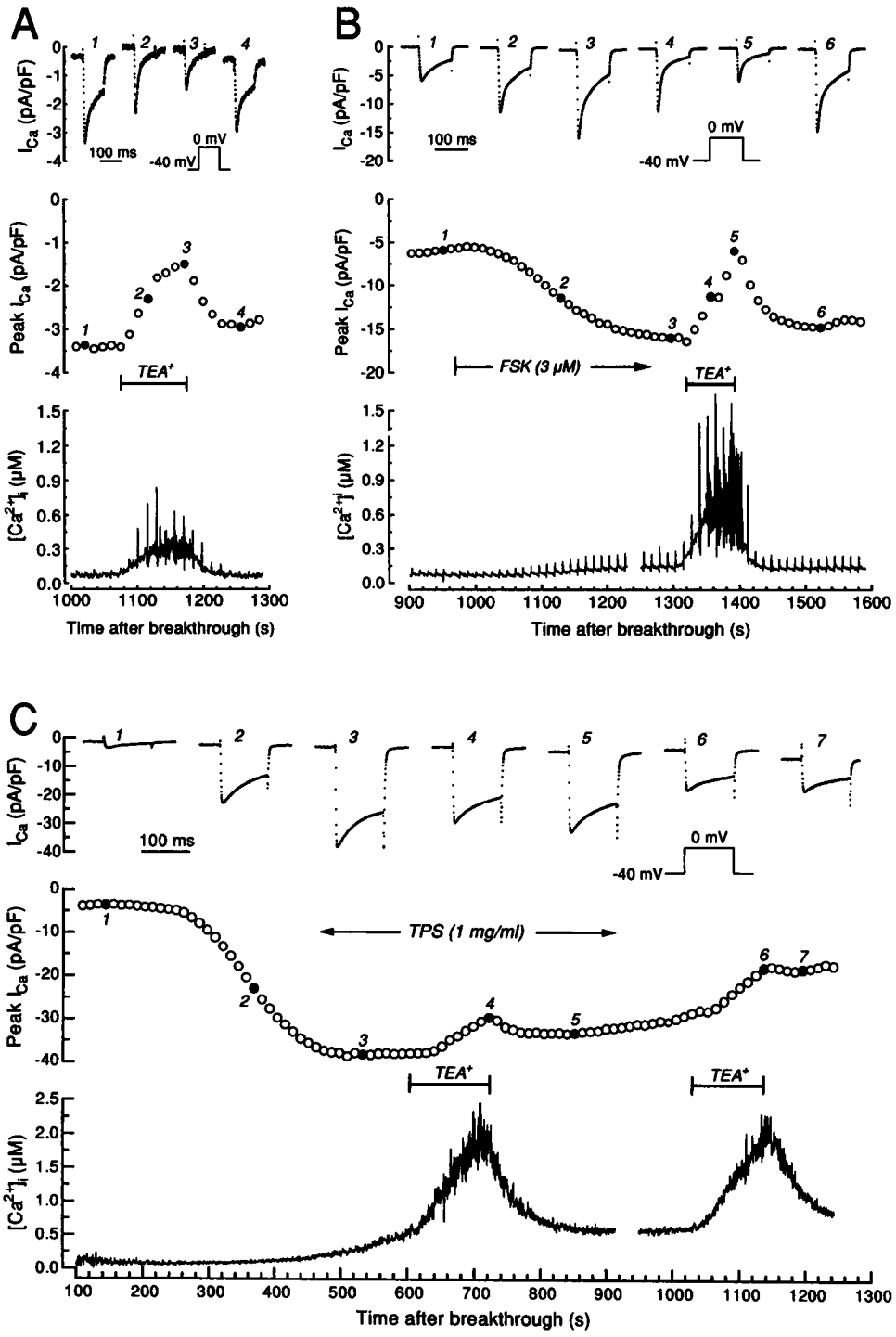

FIGURE 2 Effects of replacing extracellular sodium (Na^+_o) with TEA^+ on I_{Ca} density and $[Ca^{2+}]_i$. (*A*) A typical control response is illustrated, when the intracellular solution contained 0.2 mM EGTA (IS-B) in the absence of forskolin and trypsin; (*B*) the same intracellular solution was used. Removal of Na^+_o was proceeded by bath perfusion of 3 μM forskolin (FSK). (*C*) The intracellular solution contained 10 mM EGTA (IS-A) and 1 mg/ml trypsin (TPS). In all panels, ● in the middle panels represent the peak I_{Ca} density of the corresponding example currents shown in the top panels. (*A*) Cell Oct13A, cell capacitance 102.3 pF, access resistance 10.2 MΩ; (*B*) cell Sep13G, cell capacitance 168.3 pF, access resistance 5.8 MΩ; (*C*) cell Jul28A, cell capacitance 108.8 pF, access resistance 4.5 MΩ.

A in You et al., 1994). After augmentation of peak I_{Ca} by cell dialysis with trypsin, massive increments of $[Ca^{2+}]_i$ beyond 1.5 μM produced only minute inhibition of peak I_{Ca} (Fig. 2 *C*).

Fig. 3 summarizes the relations between average peak I_{Ca} and average $[Ca^{2+}]_i$ in control, forskolin- and trypsin-treated cells. Fig. 3 *A* illustrates the large enhancement of peak-I_{Ca} density by forskolin and especially by trypsin at all $[Ca^{2+}]_i$ studied. To better visualize the differences in peak-I_{Ca} sensitivities to $[Ca^{2+}]_i$ under these three conditions, normalized peak I_{Ca} were replotted in Fig. 3 *B*. The present control data (○) match the normalized peak I_{Ca}-$[Ca^{2+}]_i$ relation reported previously by us (You et al., 1994, $K_{0.5}$ = 60 nM). Cell dialysis with trypsin (□), and to a lesser extent bath application of forskolin (▽), shifted the peak I_{Ca}-$[Ca^{2+}]_i$ relation to the right. If we assume an increase in $K_{0.5}$ (equivalent to a decrease in sensitivity) of 20 and 3 times that of control for trypsin and forskolin, respectively, other parameters unaltered, the new peak I_{Ca}-$[Ca^{2+}]_i$ relations for trypsin (- - - -) and forskolin (· · · · ·) fit the experimental data almost perfectly.

Effects of forskolin and trypsin on $[Ca^{2+}]_i$-induced changes in I_{Ca} decay

Changes in $[Ca^{2+}]_i$ and I_{Ca} amplitude have been reported to affect the time course of I_{Ca} decay to various degrees (cf. McDonald et al., 1994). Thus, kinetic analysis of I_{Ca} inactivation may provide some insight into the mechanism for the differences in peak-I_{Ca} sensitivity to $[Ca^{2+}]_i$ under the different experimental conditions described above (e.g., Gutnick et al., 1989). A two-exponential method was used to fit the inactivation phase of I_{Ca} (Isenberg and Klöckner, 1982), from which fast (τ_F) and slow (τ_S) time constants and the respective amplitudes (A_F and A_S) were derived. From the sample current traces shown in Fig. 4 *A*, it seems that after elevation of $[Ca^{2+}]_i$ (□) and a greater portion of peak-I_{Ca} inactivated via a fast pathway (i.e., lower A_S and higher A_F values compared with control) without drastic changes in τ_F; τ_S was reduced at high $[Ca^{2+}]_i$. Forskolin application increased both A_F and A_S at low and high $[Ca^{2+}]_i$, shortened τ_S, primarily at low $[Ca^{2+}]_i$, and hardly affected τ_F at either $[Ca^{2+}]_i$ examined (Fig. 4 *B*). An increased $[Ca^{2+}]_i$-induced acceleration of τ_S was no longer apparent. Again, a greater fraction of peak I_{Ca} inactivated via a fast route at high $[Ca^{2+}]_i$, although the fractional contribution of the fast inactivation pathway to overall I_{Ca} inactivation ($A_F/(A_F + A_S)$; see Fig. 5 *C*) was less pronounced as compared with control. Trypsin dialysis moderately increased A_F and drastically augmented A_S at either $[Ca^{2+}]_i$; both τ_F and τ_S were prolonged (Fig. 4 *C*). (Although the fitting of the slowly decaying portion of I_{Ca} seems reasonable, the accuracy of determining A_S and τ_S is compromised because of the fact that they were derived from 100-ms pulses.) However, the enhancement of the fast

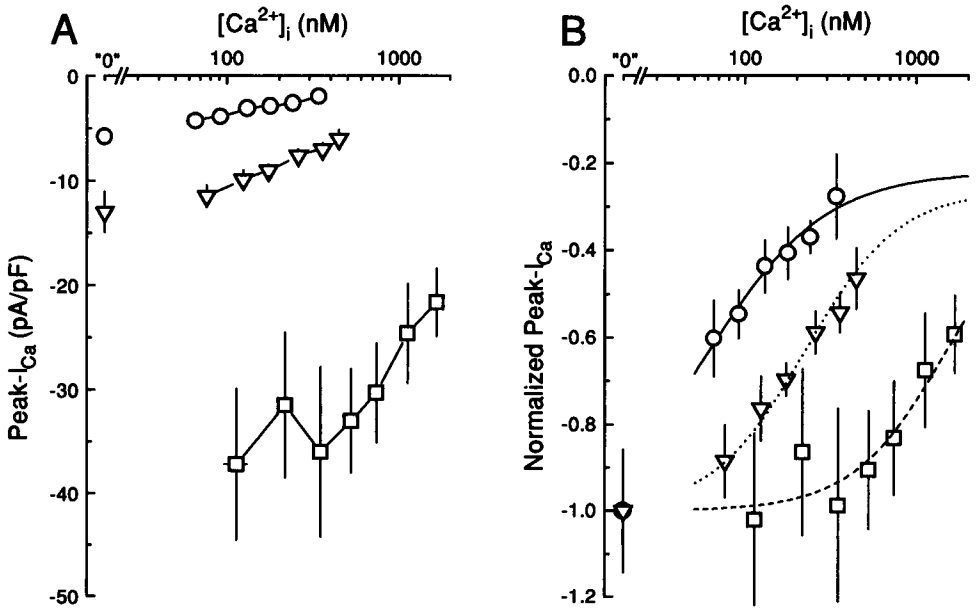

FIGURE 3 Correlation between peak I_{Ca} and $[Ca^{2+}]_i$ at 22°C. (*A*) The peak I_{Ca}-$[Ca^{2+}]_i$ relations in control (○, n = 6), forskolin-superfused (▽, n = 5), and trypsin-dialyzed (□, n = 6) cells are illustrated. Each symbol in A represents a pair of averaged peak-I_{Ca} and $[Ca^{2+}]_i$ values from a group of three to eight raw data points, all having $[Ca^{2+}]_i$ in a narrow range. Seven such $[Ca^{2+}]_i$ ranges were set for grouping of raw data points in each experimental condition. For control (○, n = 10) and forskolin (▽, n = 5), the points at x = "0" represent averaged peak I_{Ca} from experiments using 40 mM EGTA in the cell dialysate (IS-C), in which $[Ca^{2+}]_i$ was below the detection limit of Fura-2. Also note that in some cases standard errors are smaller than symbol size. (*B*) The same averaged control data (○) are overlaid with a normalized I_{Ca} -$[Ca^{2+}]_i$ relation (——), which was derived previously (You et al., 1994). The averaged data from forskolin-treated cells (▽) are overlaid with a Boltzmann function (· · · ·) having a $K_{0.5}$ three times that of control. The trypsin data (□) are overlaid with the same relation, assuming a $K_{0.5}$ 20 times that of control (- - - -).

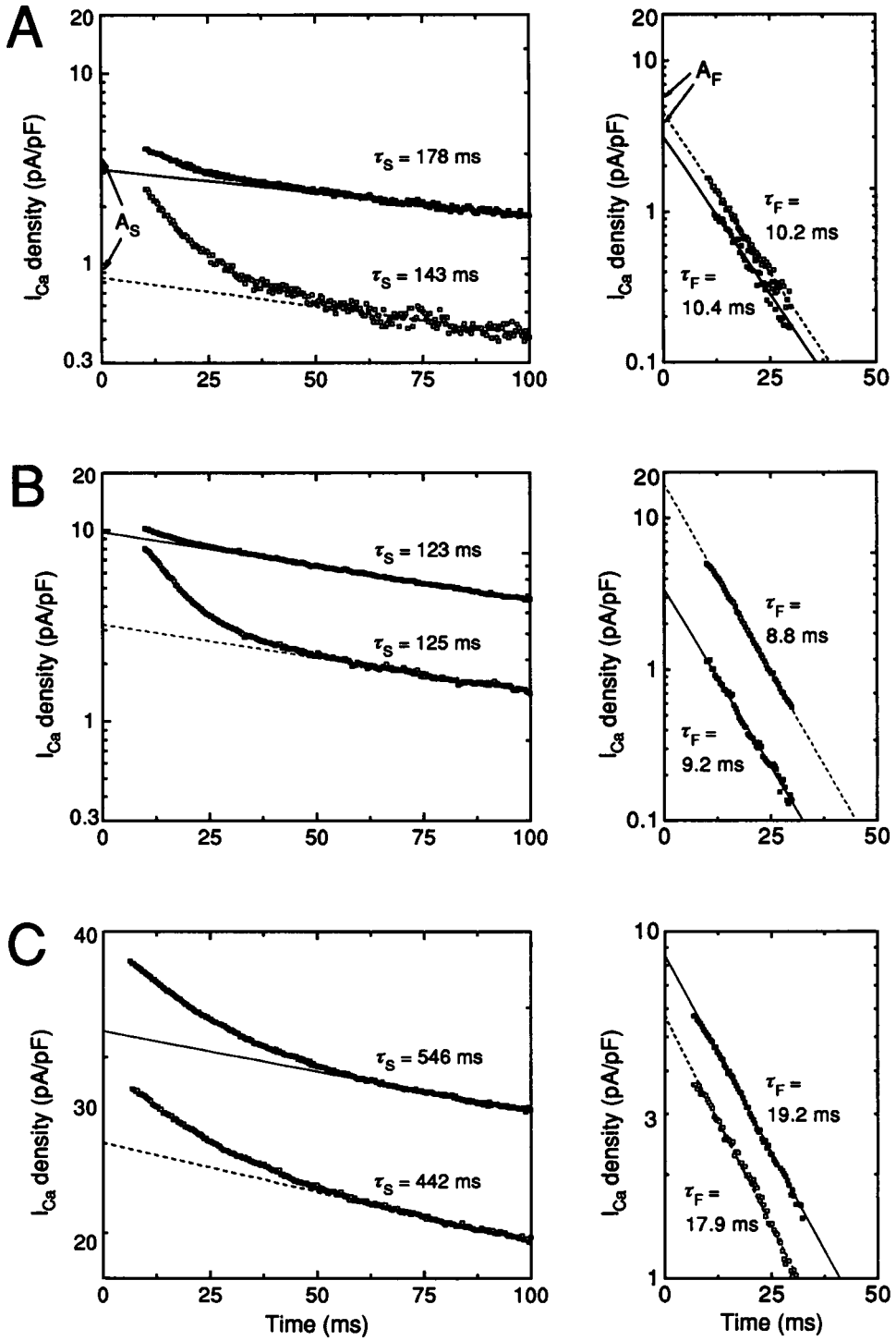

FIGURE 4 Effects of $[Ca^{2+}]_i$ on the time courses of I_{Ca} inactivation under control conditions (*A*), after forskolin application (*B*), and after trypsin dialysis (*C*). In order to derive the time constants and amplitudes of I_{Ca} inactivation, an exponential function was first fitted to the slowly decaying phase of $I_{Ca} \geq 60$ ms (*left*). The difference between this fit and early I_{Ca} was plotted in the right panels and fitted by a second exponential function (cf. Isenberg and Klöckner, 1982). Zero time represents the onset of the 100-ms-long clamp pulses from −40 mV to 0 mV. The time constants (τ_S and τ_F) and amplitudes (A_S and A_F) of I_{Ca} inactivation were derived from the slopes of the fits ($-1/\tau_{S,F}$) and their intersections with the ordinate, respectively. Shown in each panel are two current traces corresponding to I_{Ca} recorded before (■ and ——) and after (□ and - - - -) TEA^+_o-induced $[Ca^{2+}]_i$ elevation; $[Ca^{2+}]_i$ values in the respective panels are 74 and 263 nM (*A*), 71 and 339 nM (*B*), and 437 and 1820 nM (*C*), respectively.

inactivating portion of I_{Ca} by high $[Ca^{2+}]_i$ was abolished; A_F actually decreased upon increasing $[Ca^{2+}]_i$.

The average kinetics and amplitudes of I_{Ca} inactivation in relation to $[Ca^{2+}]_i$ are summarized in Fig. 5. The following points regarding τ_F and τ_S are worth noting. First, control τ_F was shortened by $[Ca^{2+}]_i$ increases between <10 and ~60 nM but was insensitive to $[Ca^{2+}]_i$ increments beyond ~60 nM (Fig. 5 *A*, ○). τ_F was also unaffected by forskolin-induced increases in Ca^{2+} influx at $[Ca^{2+}]_i > 60$ nM (Fig. 5 *A*, ▽). (Note that at $[Ca^{2+}]_i < 60$ nM, τ_F and A_F could not be determined accurately because of its negligible contribution to overall I_{Ca} inactivation (<4%) in the presence of forskolin.) Trypsin apparently antagonized the modulatory effect of increasing $[Ca^{2+}]_i$ on τ_F so that high $[Ca^{2+}]_i$ failed to accelerate τ_F under this condition (Fig. 5 *A*, □). Second, τ_S is slightly reduced by $[Ca^{2+}]_i$ elevation under control conditions (Fig. 5 *B*, ○), and by forskolin-induced increases in Ca^{2+} influx at $[Ca^{2+}]_i$ up to ~100 nM (Fig. 5 *B*, ▽).

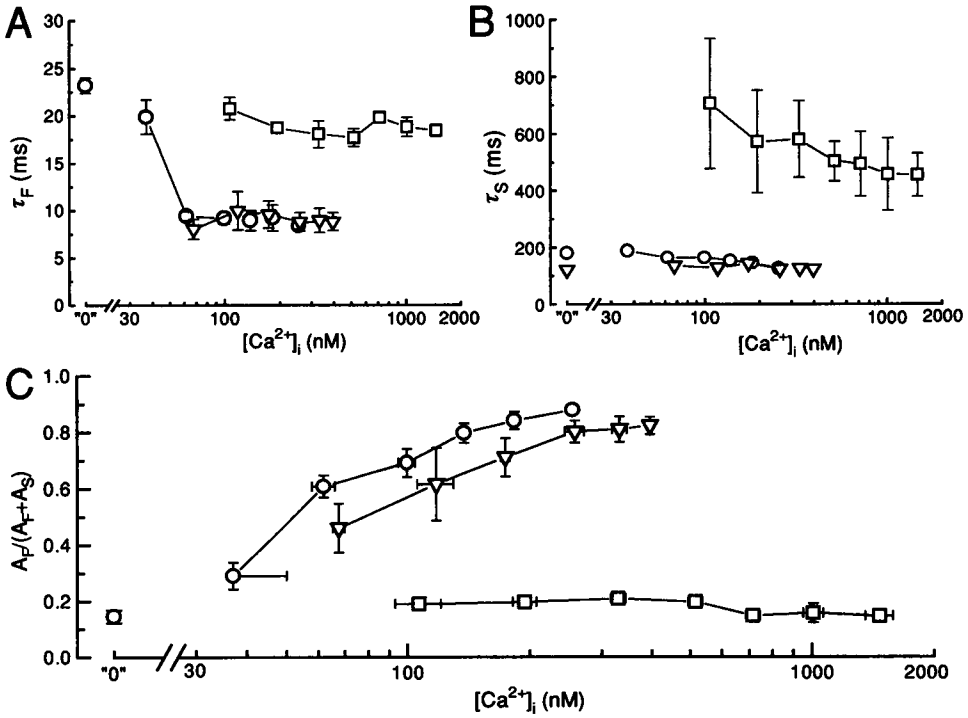

FIGURE 5 Correlation between $[Ca^{2+}]_i$ and I_{Ca} inactivation in control (○, n = 6), forskolin-superfused (▽, n = 5), and trypsin-dialyzed (□, n = 6) cells. Shown in A and B are the influences of $[Ca^{2+}]_i$ elevation on the fast (τ_F) and slow (τ_S) time constants, respectively. (*C*) The relative amplitude of fast inactivation $A_F/(A_S+A_F)$ is plotted against $[Ca^{2+}]_i$. For details on data gathering and presentation, see legend to Fig. 3. Also note that in some cases standard errors are smaller than symbol size.

However, under the latter condition, a dependence of τ_S on $[Ca^{2+}]_i$ was no longer apparent. Trypsin, on the other hand, greatly prolonged τ_S (Fig. 5 *B*, □), even though it enhanced Ca^{2+} influx far more than forskolin did.

Fig. 5 *C* illustrates the relative magnitude of fast I_{Ca} inactivation ($A_F/(A_F + A_S)$; also see Gutnick et al., 1989) at different $[Ca^{2+}]_i$. Under control conditions (○), the contribution of fast inactivation increased significantly at $[Ca^{2+}]_i$ beyond 30 nM. Compared with control, forskolin-potentiated I_{Ca} (▽) showed less inactivation via a fast kinetic pathway at comparable $[Ca^{2+}]_i$. After trypsin digestion (□), the enhancement of fast inactivation by increasing $[Ca^{2+}]_i$ was occluded.

DISCUSSION

Effects of forskolin and trypsin on I_{Ca} size, kinetics, and $[Ca^{2+}]_i$ sensitivity

Both forskolin and trypsin augmented peak I_{Ca}. However, forskolin increased peak I_{Ca} substantially less than trypsin did, which is not compatible with the idea that the action of both chemicals is on a common blocking site (e.g., Hescheler and Trautwein, 1988). Moreover, I_{Ca} was much more effectively guarded against $[Ca^{2+}]_i$-induced inhibition by trypsin than by forskolin, further suggesting different mechanisms involved.

After forskolin application and trypsin dialysis, peak I_{Ca} became 3 and 20 times less sensitive, respectively, to $[Ca^{2+}]_i$ elevation, as compared with control conditions (Fig. 3). This observation seems to be at least qualitatively related to the occlusion of a fast I_{Ca} inactivation pathway by forskolin and trypsin (Fig. 5 *C*). For control I_{Ca} (○), elevation of $[Ca^{2+}]_i$ resulted in an increase in the relative magnitude of fast inactivation ($A_F/(A_S+A_F)$, Fig. 5 *C*), although τ_F was insensitive to $[Ca^{2+}]_i$ changes in this range (Fig. 5 *A*). Forskolin-stimulated I_{Ca} (▽) showed less sensitivity of $A_F/(A_s+A_F)$ to $[Ca^{2+}]_i$, whereas trypsin (□) completely abolished the enhancement of fast inactivation by $[Ca^{2+}]_i$ (Fig. 5 *C*). Because τ_F is of similar duration as time-to-peak I_{Ca} (~10 ms, cf. Fig. 4), the fast inactivation process may contribute to the reduction of peak I_{Ca} by inactivating Ca^{2+} channels before channel opening is complete, thus reducing I_{Ca} amplitude. This suggestion is supported by the notable increase in the incidence of blank single Ca^{2+} channel sweeps after an elevation of $[Ca^{2+}]_i$ beyond the stimulatory range (Hirano and Hiraoka, 1994; their Fig. 11 *B* and *C*, c). At the single Ca^{2+} channel level, the primary action of forskolin and trypsin is the reduction of the probability to record empty single-channel current traces upon depolarization, which results in an increase of ensemble average Ca^{2+} current amplitude (cf. McDonald et al., 1994). This cessation of Ca^{2+} channel entry into states of unavailability (cf. Cavalié et al., 1986) may form the basis for the reduced sensitivity of peak I_{Ca} to $[Ca^{2+}]_i$-induced inhibition.

According to Giannattasio et al. (1991), the fast and slow components of I_{Ca} inactivation in A7r5 smooth muscle cells reflect Ca^{2+}-dependent and voltage-dependent inactivation, respectively. In guinea pig ventricular myocytes, however, τ_S seems to be Ca^{2+}-dependent as well. Under control conditions, τ_S became shorter as $[Ca^{2+}]_i$ was increased (Fig. 5 *B*). The τ_S after forskolin application at 40 mM internal EGTA (Fig. 5 *B*, x = "0") was significantly shorter than its

corresponding control value ($p < 0.01$). As $[Ca^{2+}]_i$ was less than 10 nM under both experimental conditions, τ_S apparently was shortened as a result of increased Ca^{2+} influx by forskolin. Under this condition, the dependence of τ_S on $[Ca^{2+}]_i$ was no longer apparent. At the single Ca^{2+} channel level, an acceleration of τ_S would correspond to an abbreviation of channel activity in traces with channel openings (Cavalié et al., 1986). Indeed, such a curtailment of single-channel activity during depolarization was observed with increased bulk $[Ca^{2+}]_i$ in cardiac L-type Ca^{2+} channels incorporated into planar lipid bilayers (Haack and Rosenberg, 1994), as well as after local $[Ca^{2+}]_i$ increments due to prior Ca^{2+} entry during a prepulse in cell-attached patches from rat ventricular cardiomyocytes (Imredy and Yue, 1994). Trypsin greatly hindered the slow inactivation process, even though Ca^{2+} flux increased more than sevenfold (Fig. 5 *B*). The very slow τ_S left behind after trypsin dialysis may primarily reflect voltage-dependent inactivation, as seen in the inactivation of Ba^{2+} current through Ca^{2+} channels (McDonald et al., 1986).

Under control conditions, shortening of τ_F occurred when $[Ca^{2+}]_i$ increased from <10 nM to ~60 nM (Fig. 5 *A*), suggesting a high apparent affinity for cytoplasmic Ca^{2+}. In addition, τ_F was largely unaffected by phosphorylation and the resultant increase in I_{Ca} during bath perfusion of 3 μM forskolin at the $[Ca^{2+}]_i$ examined (Fig. 5 *A*), so that it is likely not flux-dependent. The high apparent sensitivity of τ_F to $[Ca^{2+}]_i$ was completely removed by trypsin, although the basal τ_F remained intact (Fig. 5 *A*).

In summary, the above discussion shows a qualitative relation between changes in the amplitudes of the respective components of I_{Ca} inactivation and changes in peak I_{Ca} amplitude with variations of bulk $[Ca^{2+}]_i$ under the three experimental conditions examined. These findings are compatible with a $[Ca^{2+}]_i$-induced shift of channel gating to a low (or zero) open probability mode, with cAMP-dependent phosphorylation and tryptic digestion occluding this transition to various degrees. In the context of a differential contribution of changes in local versus bulk $[Ca^{2+}]_i$ to changes in peak I_{Ca} and inactivation time constants, the following two observations at the single Ca^{2+} channel level are worth noting. First, local $[Ca^{2+}]_i$ increments close to the inner mouth of the Ca^{2+} channel enhance the decay of open probability conditioned on first openings during test pulses (Yue et al., 1990; Imredy and Yue, 1994), as changes in bulk $[Ca^{2+}]_i$ do (Haack and Rosenberg, 1994). Second, local $[Ca^{2+}]_i$ elevations slow the latencies to first channel opening, which reduces peak current amplitude (Imredy and Yue, 1994), as an increased incidence for blank single-channel current traces by elevated bulk $[Ca^{2+}]_i$ does (Hirano and Hiraoka, 1994). Thus, it seems that changes in local and bulk $[Ca^{2+}]_i$ qualitatively result in similar changes of whole-cell I_{Ca} size and kinetics, although the respective changes potentially differ quantitatively.

Supposed model of $[Ca^{2+}]_i$-mediated inhibition of I_{Ca}

The present results are most compatible with models in which it is assumed that Ca^{2+} channels can exist in two modes that are in equilibrium with one another (Fig. 6; cf. Bean, 1989; Imredy and Yue, 1994). In the "willing" mode, predominant at low $[Ca^{2+}]_i$, after forskolin-induced maximal cAMP-dependent phosphorylation or tryptic disruption of inactivation processes, channels can be opened effectively by depolarization, which results in high open-probability single-channel current records, short latencies to first channel opening, a high probability of reopening, and a low percentage of single channel current traces without open-

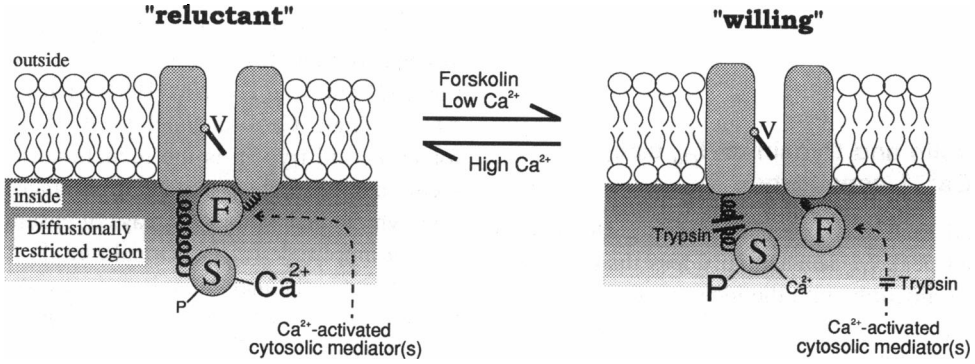

FIGURE 6 Proposed model of $[Ca^{2+}]_i$-mediated inhibition of I_{Ca}. $[Ca^{2+}]_i$-dependent inactivation of the Ca^{2+} channel is brought about by two "ball-and-chain" structures connected to the inner mouth region of the Ca^{2+} channel. The "fast ball" (*F*), attached to the channel via a short chain, contains neither Ca^{2+}-binding nor phosphorylation sites. It seems, however, indirectly turned on by elevation of $[Ca^{2+}]_i$. The "slow ball" (*S*), which partially protrudes out of the diffusionally restricted region, contains a Ca^{2+}-binding site (Ca^{2+}) and a phosphorylation site (*P*). The Ca^{2+}-binding site is accessible to both cytosolic Ca^{2+} and Ca^{2+} in the diffusionally restricted space; binding of Ca^{2+} accelerates the inactivation. Cyclic AMP-dependent phosphorylation allosterically decreases the affinity of the Ca^{2+} binding site for Ca^{2+}. Phosphorylation also compromises fast inactivation by potentially bringing the "slow ball" (*S*) closer to the channel, thus limiting the movement of the "fast ball" (*F*). Both fast and slow inactivation particles apparently are susceptible to tryptic digestion, either indirectly by blocking the action of a $[Ca^{2+}]_i$-dependent cytoplasmic activator or directly by clipping a chain. The voltage-dependent inactivation gate (*V*) seems to be hidden inside the conductive pore. See Discussion section for further details.

ings. In the "reluctant" mode, predominant at high $[Ca^{2+}]_i$ and basal cAMP-dependent phosphorylation, channels are not opened easily by depolarization, resulting in low open-probability single-channel current sweeps, long latencies to first channel opening, a low probability of reopening, and a high percentage of single-channel current records without openings. It is postulated that L-type Ca^{2+} channels interconvert between the two modes and that an elevation in $[Ca^{2+}]_i$ places a larger fraction of channels in the reluctant mode. This translocation of Ca^{2+} channels into the reluctant pool is effectively hindered by cAMP-dependent phosphorylation and largely occluded by tryptic digestion.

In our basic model (Fig. 6), inactivation particles are represented by "ball-and-chain" structures as the physical entities for the slow (A_S, τ_S) and fast (A_F, τ_F) inactivation gates (cf. Armstrong and Bezenilla, 1977). Although the ball-and-chain theory of inactivation has been unequivocally proven only for *Shaker* K^+ channels (Hoshi et al., 1990, 1991), the similarity in primary structure and proposed folding pattern of primary amino acid repeats between the functional K^+ and Ca^{2+} channel subunits (Catterall, 1988) renders this assumption for Ca^{2+} channels not entirely implausible. Two balls are connected to the inner mouth region of the Ca^{2+} channel via two chains of different lengths. Under basal conditions (Fig. 6, *left*), an increase in $[Ca^{2+}]_i$ moves both the fast (F) and the slow (S) inactivation particle faster into an occluding position, thus placing a larger fraction of Ca^{2+} channels more rapidly in a reluctant mode. Because τ_F is insensitive to increased Ca^{2+} flux after cAMP-dependent phosphorylation, at least beyond a $[Ca^{2+}]_i$ of ~60 nM, this process is unlikely to be regulated by direct binding of Ca^{2+}. It may be modulated by an indirect (cytoplasmic?) mechanism other than cAMP-dependent phosphorylation, which is sensitive to $[Ca^{2+}]_i$ in the tens of nanomolar range. A possible cytoplasmic site has also been suggested in a recent report by Sipido et al. (1995) to account for the inhibition of I_{Ca} during Ca^{2+} release from the sarcoplasmic reticulum. On the other hand, maximal cAMP-dependent phosphorylation of a site at the slow inactivation particle (P) close to the Ca^{2+} binding site (Ca^{2+}) allosterically decreases the affinity for Ca^{2+} binding and possibly compromises the $[Ca^{2+}]_i$-induced fast closing of the Ca^{2+} channel by causing a conformational change in the quaternary stucture of the slow ball-and-chain type structure. The latter potentially brings the phosphorylated "slow ball" (S) closer to the conductive pore, thus hindering the movement of the "fast ball" (F) (Fig. 6, *right*). Both processes taken together would place a larger fraction of Ca^{2+} channels in the willing mode. Finally, trypsin apparently disrupts most of the modulation of the fast and slow balls by nanomolar $[Ca^{2+}]_i$ readily placing affected channels in the willing mode (Fig. 6, *right*).

Physically, the "slow ball-long chain" inactivation particle could be part of the C-terminal end of the Ca^{2+} channel α_1-subunit, as the primary structure of this region of the Ca^{2+} channel protein contains the consensus sites for cAMP-dependent phosphorylation and Ca^{2+} binding (cf. Mikami et al., 1989). Support for this suggestion comes from the observation that the truncated form of the α_1-subunit (De Jongh et al., 1991), which lacks the final 211 COOH-terminal amino acids (Beam et al., 1992), lacks Ca^{2+}-dependent inactivation when expressed in dysgenic myotubes (Tanabe et al., 1990). The short cytoplasmic loop between repeats II and III of the α_1-subunit may represent a suitable physical candidate for the "fast ball-short chain" inactivation particle. Finally, the structure responsible for voltage-dependent inactivation (V, Fig. 6) seems to be hidden deep inside the channel pore.

We thank Mr. Darren J. Cole for excellent technical assistance, Mr. Brian K. Hoyt for unfailing electronic and computer support, and Mr. Colin F. Foley for valuable suggestions on the final version of the manuscript. This work was supported by Grants MRC DG-396 and MRC MT-11849 from the Medical Research Council of Canada.

REFERENCES

Armstrong, C. M., and F. Bezanilla. 1977. Inactivation of the sodium channel. II. Gating current experiments. *J. Gen. Physiol.* 70:567–590.

Armstrong, C. M., F. Bezanilla, and E. Rojas. 1973. Destruction of sodium conductance inactivation in squid axons perfused with pronase. *J. Gen. Physiol.* 62:375–391.

Beam, K. G., B. A. Adams, T. Niidome, S. Numa, and T. Tanabe. 1992. Function of a truncated dihydropyridine receptor as both voltage sensor and calcium channel. *Nature (Lond.).* 360:169–171.

Bean, B. P. 1989. Neurotransmitter inhibition of neuronal calcium currents by changes in channel voltage dependence. *Nature (Lond.).* 340: 153–156.

Catterall, W. A. 1988. Structure and function of voltage-sensitive ion channels. *Science.* 242:50–61.

Cavalié, A. D., D. Pelzer, and W. Trautwein. 1986. Fast and slow gating behaviour of single calcium channels in cardiac cells. Relation to activation and inactivation of calcium-channel current. *Pflügers Arch.* 406: 241–258.

De Jongh, K. S., C. Warner, A. A. Colvin, and W. A. Catterall. 1991. Characterization of the two size forms of the α1 subunit of skeletal muscle L-type calcium channels. *Proc. Natl. Acad. Sci. USA.* 88: 10778–10782.

Giannattasio, B., S. W. Jones, and A. Scarpa. 1991. Calcium currents in the A7r5 smooth muscle-derived cell line: calcium-dependent and voltage-dependent inactivation. *J. Gen. Physiol.* 98:987–1003.

Gutnick, M. J., H. D. Lux, D. Swandulla, and H. Zucker. 1989. Voltage-dependent and calcium dependent inactivation of calcium channel current in identified snail neurones. *J. Physiol. (Lond.).* 412:197–220.

Haack, J. A., and R. L. Rosenberg. 1994. Calcium-dependent inactivation of L-type calcium channels in planar lipid bilayers. *Biophys. J.* 66: 1051–1060.

Hadley, R. W., and W. J. Lederer. 1991. Ca^{2+} and voltage inactivate Ca^{2+} channels in guinea-pig ventricular myocytes through independent mechanisms. *J. Physiol. (Lond.).* 444:257–268.

Hamill, O. P., A. Marty, E. Neher, B. Sakmann, and F. J. Sigworth. 1981. Improved patch-clamp techniques for high-resolution current recording from cells and cell-free membrane patches. *Pflügers Arch.* 391:85–100.

Hescheler, J., and W. Trautwein. 1988. Modification of L-type calcium current by intracellularly applied trypsin in guinea-pig ventricular myocytes. *J. Physiol. (Lond.).* 404:259–274.

Hirano, Y., and M. Hiraoka. 1994. Dual modulation of unitary L-type Ca^{2+} channel currents by $[Ca^{2+}]_i$ in Fura-2-loaded guinea-pig ventricular myocytes. *J. Physiol. (Lond.).* 480.3:449–463.

Hoshi, T., W. N. Zagotta, and R. W. Aldrich. 1990. Biophysical and molecular mechanisms of *Shaker* potassium channel inactivation. *Science.* 250:533–538.

Hoshi, T., W. N. Zagotta, and R. W. Aldrich. 1991. Two types of inactivation in *Shaker* K^+ channels: effects of alterations in the carboxy-terminal region. *Neuron.* 7:547–556.

Imredy, J. P., and D. T. Yue. 1994. Mechanism of Ca^{2+}-sensitive inactivation of L-type Ca^{2+} channels. *Neuron.* 12:1301–1318.

Isenberg, G., and U. Klöckner. 1982. Calcium currents of isolated bovine ventricular myocytes are fast and of large amplitude. *Pflügers Arch.* 395:30–41.

Kirsch, G. E., and A. M. Brown. 1989. Trypsin activation of atrial muscarinic K^+ channels. *Am. J. Physiol.* 257:H334–H338.

McDonald, T. F., A. Cavalié, W. Trautwein, and D. Pelzer. 1986. Voltage-dependent properties of macroscopic and elementary calcium channel currents in guinea pig ventricular myocytes. *Pflügers Arch.* 406: 437–448.

McDonald, T. F., S. Pelzer, W. Trautwein, and D. J. Pelzer. 1994. Regulation and modulation of calcium channels in cardiac, skeletal, and smooth muscle cells. *Physiol. Rev.* 74:365–507.

Mikami, A., K. Imoto, T. Tanabe, T. Niidome, Y. Mori, H. Takeshima, S. Narumiya, and S. Numa. 1989. Primary structure and functional expression of the cardiac dihydropyridine-sensitive calcium channel. *Nature (Lond.).* 340:230–233.

Obejero-Paz, C. A., S. W. Jones, and A. Scarpa. 1991. Calcium currents in the A7r5 smooth muscle-derived cell line: increase in current and selective removal of voltage-dependent inactivation by intracellular trypsin. *J. Gen. Physiol.* 98:1127–1140.

Sipido, K. R., G. Callewaert, and E. Carmeliet. 1995. Inhibition and rapid recovery of Ca^{2+} current during Ca^{2+} release from sarcoplasmic reticulum in guinea pig ventricular myocytes. *Circ. Res.* 76:102–109.

Tanabe, T., A. Mikami, S. Numa, and K. G. Beam. 1990. Cardiac-type excitation-contraction coupling in dysgenic skeletal muscle injected with cardiac dihydropyridine receptor cDNA. *Nature (Lond.).* 344:451–453.

You, Y., D. J. Pelzer, and S. Pelzer. 1994. Modulation of calcium current density by intracellular calcium in isolated guinea pig ventricular cardiomyocytes. *Biochem. Biophys. Res. Commun.* 204:732–740.

Yue, D. T., P. H. Backx, and J. P. Imredy. 1990. Calcium-sensitive inactivation in the gating of single calcium channels. *Science.* 250: 1735–1738.